



**HAL**  
open science

## Pillar burst assessment based on large-scale numerical modeling

Samar S. Ahmed, Marwan Al Heib, Yann Gunzburger, Vincent Renaud

► **To cite this version:**

Samar S. Ahmed, Marwan Al Heib, Yann Gunzburger, Vincent Renaud. Pillar burst assessment based on large-scale numerical modeling. ISRM European Rock Mechanics Symposium (EUROCK 2017), Jun 2017, Ostrava, Czech Republic. pp.179-187, 10.1016/j.proeng.2017.05.170 . ineris-01864661

**HAL Id: ineris-01864661**

**<https://ineris.hal.science/ineris-01864661>**

Submitted on 30 Aug 2018

**HAL** is a multi-disciplinary open access archive for the deposit and dissemination of scientific research documents, whether they are published or not. The documents may come from teaching and research institutions in France or abroad, or from public or private research centers.

L'archive ouverte pluridisciplinaire **HAL**, est destinée au dépôt et à la diffusion de documents scientifiques de niveau recherche, publiés ou non, émanant des établissements d'enseignement et de recherche français ou étrangers, des laboratoires publics ou privés.



Symposium of the International Society for Rock Mechanics

## Pillar Burst Assessment Based on Large-Scale Numerical Modeling

Samar S. Ahmed<sup>a,c\*</sup>, Marwan ALHeib<sup>b</sup>, Yann Gunzburger<sup>a</sup>, Vincent Renaud<sup>b</sup>

<sup>a</sup> GeoResources, Ecole des Mines de Nancy, Université de Lorraine, Nancy, 54042, France

<sup>b</sup> INERIS, Ecole des Mines de Nancy, Nancy, 54042, France

<sup>c</sup> Mining department, Faculty of engineering, Cairo university, Cairo, 54042, Egypt

### Abstract

Stress concentration is a direct result of stress redistribution around an excavation, that may lead to rock bursting under specific geomechanical conditions. This paper presents a case-study of a rockburst that took place in the shaft station area of the Provence coal mine in Southern France. The mined coal seam has a 2.5 m thickness and a 10° dip angle. The rockburst occurred in 1993 at the shaft station level, where it is surrounded by several longwall panels that were excavated between 1984 and 1994. The area of the shaft station is at 1000 m depth. A very thin layer of stiff limestone occupied the middle of the exploited coal seam. A large-scale finite difference numerical model of the mine has been constructed by using FLAC<sup>3D</sup>. The model simulates the area of the shaft with its irregular pillars and the longwall panels excavated between 1984 and 1993. The excavations were performed in two steps. Firstly, the galleries of the shaft station area were excavated in order to determine their effect on the failed pillar. Then, the longwall panels were excavated year by year to detect the stress and strain energy increments induced on the pillars. The origin of the rockburst was analysed based on different rockburst criteria. The results show that the vertical stress increased in the shaft station pillars due to excavation of longwall panels. In addition, we found that the small pillars have higher burst tendency than the large ones. Finally, the Burst Potential Index (*BPI*) was found to be able to estimate the pillar burst tendency based on the energy storage rate (*ESR*), however, this criterion (*BPI*) is based on calculating the stress and the energy changes in the vertical direction only.

© 2017 The Authors. Published by Elsevier Ltd. This is an open access article under the CC BY-NC-ND license (<http://creativecommons.org/licenses/by-nc-nd/4.0/>).

Peer-review under responsibility of the organizing committee of EUROCK 2017

**Keywords:** Rockburst; Stress redistribution; Room-and-pillar; Longwall panels; Numerical modeling; Stored strain energy

\* Corresponding author. Tel.: +33-752-928-564.

E-mail address: [samar\\_\\_sayed@hotmail.com](mailto:samar__sayed@hotmail.com); [samar.sayed.ahmed@gmail.com](mailto:samar.sayed.ahmed@gmail.com)

## 1. Introduction

The most probable underground instability during room-and-pillar mining is the pillar failure. Two major types of pillar failure; i) structurally controlled failure; and ii) progressive failure. Structurally controlled failure happens when a rockmass contains planes of failure (i.e. discontinuities) and the pillars are oriented unfavorably with respect to those planes of failure. This type of failure could be easily observed. Progressive failure happens where the pillar skin has little horizontal confinement and high vertical stresses. Initially the pillar remains intact and retains its bearing capacity, then, as the spalling takes place, the stresses redistribute and reach up to the pillar core progressively until it reaches a critical cross-section area and it fails. This failure could occur in a violent brittle manner which is called pillar burst, which is a type of rockburst. In order to assess pillar failure tendency, the Factor of Safety (F.S = pillar strength/average pillar stress) is used to assess pillars stability. Many authors tried to develop empirical formulas of coal pillar strength. For example, Salamon and Munro [1] studied 125 pillars in the South African coal fields, Eq. (1) is developed to assess the coal pillar strength.

$$\sigma_{ps} = K \left( \frac{w^b}{h^a} \right) \quad (1)$$

where  $K$  is the strength of a unit cube of coal,  $\sigma_{ps}$  is the pillar strength in (MPa),  $w$  is the pillar width,  $h$  is the pillar height and  $a$  and  $b$  are empirical constants. Salamon and Munro [1] determined values 0.66 and 0.46 for  $a$  and  $b$  constants respectively and  $K$  was determined to be equal to 7.2 MPa.

However, The Factor of Safety was found to be insufficient to express coal pillars instability in case of mines with complex geometry where pillars are irregular in shape and volume. For that, recently, the rockburst criteria are used to express pillars instability in deep underground mines. Many authors developed rockburst criteria to predict the rockburst tendency in underground mines.

### 1.1. Brittleness coefficient ( $B$ )

Qiao and Tian [2] carried out an experimental study to estimate rockburst tendency by using the brittleness coefficient ( $B$ ), which is independent of in-situ stress field. The  $B$  coefficient is equal to the ratio between uniaxial compressive strength ( $\sigma_c$ ) and tensile strength ( $\sigma_t$ ) as shown in Eq.(2) The brittleness coefficient has been reported by Peng and Wang [3] and Cai et al. [4] as well.

$$B = \frac{\sigma_c}{\sigma_t} \quad (2)$$

The rockburst tendency has been classified according to the  $B$  value as:

- I. No rockburst:  $B > 40$ .
- II. Weak rockburst:  $26.7 < B \leq 40$ .
- III. Moderate rockburst:  $14.5 \leq B \leq 26.7$ .
- IV. Strong rockburst:  $B < 14.5$ .

### 1.2. Tao discriminant index ( $\alpha$ )

Tao [5] developed the Tao discriminant index ( $\alpha$ ), which is mainly based on the stress reduction factor reported in the (Q) rockmass classification system developed by Barton et al. [6]. Tao [5] suggested that his discriminant index could be calculated as follow:

$$\alpha = \frac{\sigma_c}{\sigma_1} \quad (3)$$

where  $\sigma_1$  is the maximum in-situ principal stress and  $\sigma_c$  is the unconfined compressive strength. Tao index has classified the rockburst tendency as follow:

- I. No rockburst:  $\alpha > 14.5$ .
- II. Weak rockburst:  $5.5 < \alpha \leq 14.5$ .
- III. Moderate rockburst:  $2.5 \leq \alpha \leq 5.5$ .
- IV. Strong rockburst:  $\alpha < 2.5$ .

### 1.3. Burst Potential Index (BPI)

Mitri et al. [7] developed the burst potential index (BPI), which is based on the energy storage rate (ESR) within the rock mass. The BPI could be expressed as:

$$BPI = \left( \frac{ERS}{e_c} \right) * 100\% \quad (4)$$

$$SR = \frac{d}{dV} (e_1 + e_2) \quad (5)$$

$$e_1 = \frac{1}{2} \int \varepsilon_1^T \sigma_{ind} dV \quad (6)$$

$$e_2 = \frac{1}{2} \int \varepsilon_1^T \sigma_o dV \quad (7)$$

$$e_c = \int_0^{\varepsilon_p} \sigma d\varepsilon \quad (8)$$

where  $\sigma_o$  is the in-situ stress,  $e_2$  is the strain energy caused by the in-situ stress,  $\sigma_{ind}$  is the induced stress due to mining and  $e_1$  is the strain energy due to the induced stress. Mitri et al. [7] defined the critical energy density values,  $e_c^*$ , as the area under the stress-strain curve up to the point of the peak stress as shown in Fig. 1, while  $\varepsilon_p$  is the uniaxial peak strain. In case of the absence of the stress-strain data of the rock material,  $e_c$  has been approximated by  $\frac{\sigma_c^2}{2E}$ , where  $\sigma_c$  is the material's compressive strength.

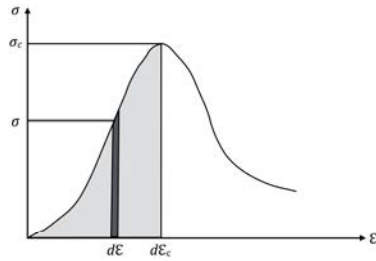


Fig. 1. Definition of critical strain energy stored in uniaxial test.

**2. Case study (the Provence coal mine)**

The present case study concerns the western part of the Provence coal mine, which is located in the South of France. It had been in operation from 1984 until 1994 using the longwall mining method as shown in Fig. 2. The shaft station area of the mine was exploited before the longwall panels by using room-and-pillar mining method (Fig. 2). The average thickness of the exploited coal seam is  $t = 2.5$  m at depth of 700 m to 1300 m (the coal seam dips  $10^\circ$ ). The shaft station is found at depth 1000 m from the earth’s surface. The overburden is mainly composed from Fuvelian limestone and Begudo-Rognacian limestone and marl as shown in Fig. 3. Below the coal seam, the rockmass contains Jurassic limestone in majority (Fig. 3). It had been found that the coal pillars in the shaft station contain a stiff limestone seam with maximum thickness 50 cm at their middle. Table 1 shows the average rockmass mechanical properties for each rock layer (Ahmed [8]). The rockmass properties were estimated based on laboratory tests.

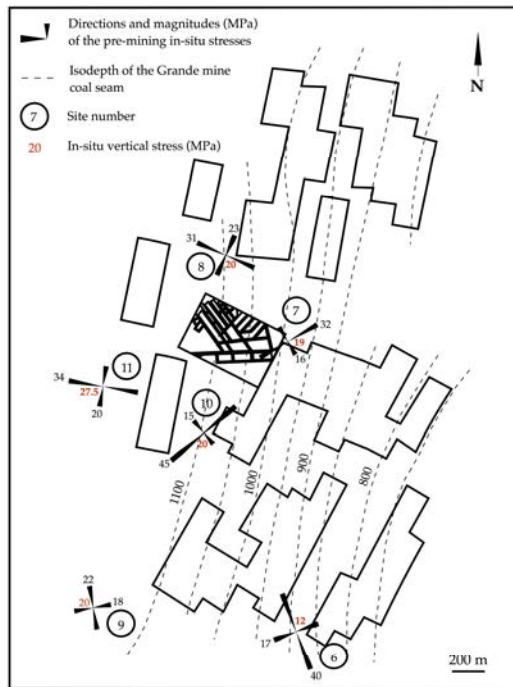


Fig. 2. Layout of the western part of the Provence coal mine (shaft station and longwall panels (1984-1994)).

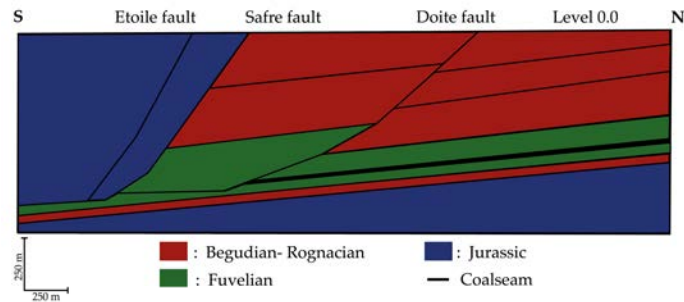


Fig. 3. Geological cross section of the mined area.

On October 1993, a rockburst of 2.7 magnitude (weak to strong rockburst on Richter scale, Bieniawski [9]) was recorded in the main shaft station area “Yvon Morandat shaft” in the Provence coal mine. The reported damage was limited to a single pillar, known as RC2 pillar. This pillar was the smallest one of the coal pillars at this area.

Table 1. Average rockmass mechanical properties Ahmed [8].

Rock types	Density (kg/m <sup>3</sup> )	UCS (MPa)	T (MPa)	Erockmass (MPa)	Poisson ratio	Friction angle (°)	Cohesion (MPa)	Brittleness coefficient (B)
Lignite coal	1500	28	1	2000	0.3	30	2.11	28
Limestone seam (50 cm)	2400	80	3.17	23000	0.1	35	5.6	25
Fuvelian limestone	2400	-	-	8450	0.2	-	-	-
Rognacian limestone	2400	-	-	1000	0.25	-	-	-
Jurassic limestone	2400	-	-	17000	0.25	-	-	-

Where UCS is the unconfined compressive strength (MPa) and T is the tensile strength.

In the current research, we tried to use the numerical modeling tool to explain the influence of longwall panels excavation on the adjacent shaft station in case of the Provence coal mine. Also, we investigated the relation between the pillar volume and its failure tendency. The rockburst criteria were used as useful tool to back-analyze the rockburst tendency in the shaft station area.

### 3. Numerical model

Many analysis and investigations were carried out by using 2D numerical modeling to understand the origin of RC2 pillar burst (Tinucci [10]) in the shaft station area. But, such 2D models did not able to describe efficiently the causes behind such brittle failure because many factors were not taken into consideration such as the third dimension, the pillar irregularity and its relevance to the surrounding pillars. Here, we exploited the evolution of the numerical modeling software to perform advanced numerical calculations to re-investigate the Provence coal mine.

A 3D numerical model of the mine was constructed using the finite difference code FLAC<sup>3D</sup> (Fig. 4). This model contains approximately 2.5 million mesh elements. Mesh density was adjusted to be fine close to the excavated area and it was increased by ratio 1.2 until model borders. Four different rock types were specified: the coal seam, the Fuvelian limestone (400 m), the Rognacian limestone (600 m) above and the Jurassic limestone beds below the coal seam. The overall dimensions of the model are 4600 m in the x- direction, 6020 m in the y-direction and 2270 m in the vertical direction (z) (Fig. 4). The top of the model coincides with the ground surface at level z=0.0 (Fig. 4). The model boundaries are fixed except the top. The vertical stress within the model is equal to the overburden weight.

Based on the pre-mining in-situ measurements provided by Gaviglio et al. [11] (Fig. 2), Ahmed et al. 2016 [12] developed a methodology to initiate the stress state within numerical modeling of the Provence coal mine case.

This stress initialization method is based on developing 3D stress gradients for all stress components as shown in Table 2.

Firstly, the galleries of the shaft station were excavated to observe their influence on the coal pillars specially RC2 pillar (the failed pillar). Then, the longwall panels were excavated from 1984 until 1993 to observe the stress changes on the shaft station area. Mohr-Coulomb mechanical model was used to express the mechanical behavior of rocks in the shaft station area (the mechanical properties of coal and thin limestone seam are as shown in Table 1). To distinguish between the shaft station pillars, the volume of plastic zones at pillars skin was recognized for each pillar. After that, the three rockburst criteria (Brittleness coefficient ( $B$ ), Tao discriminant index ( $\alpha$ ) and Burst Potential Index ( $BPI$ )) were implemented within the large-scale model to test the pillar burst tendency of RC2 pillar and 8 of its neighbors the shaft area due to longwall panels excavations.

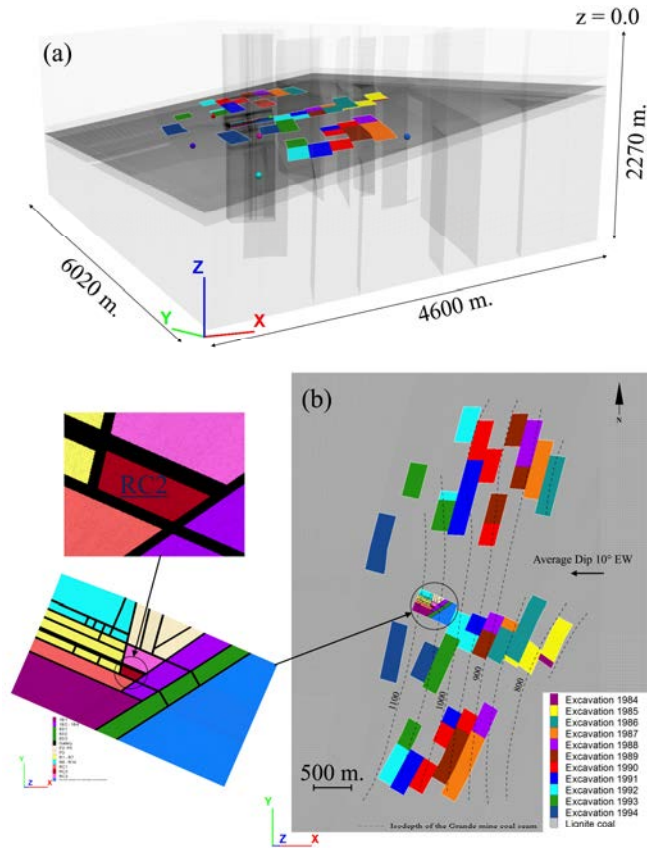


Fig. 4. The numerical model (a) 3D view of the entire model; (b) Layout of the shaft station area and the panels excavated (1984 – 1994).

Table 2. Stress components used for obtaining pre-mining stresses in the numerical model, Ahmed et al. 2016 [11].

Stress (MPa) at (x=0, y=0, z=0)		Stress gradient (MPa/m)		
		$g_x$	$g_y$	$g_z$
$\sigma_{xx}$	-0.01	-0.001161949	-0.003782241	0.016605096
$\sigma_{yy}$	-0.01	-0.005751366	0.003311549	0.019425072
$\sigma_{zz}$	0.01	0.005434012	-0.001684345	0.023544
$\sigma_{xy}$	0.01	-0.003311549	0.001161949	0.0

#### 4. Results and discussion

The galleries between pillars were excavated firstly, then the longwall panels were excavated to observe their effect on the shaft station pillars. The numerical results show that the vertical stress increased by 1.5 times its initial value. We noticed that, after galleries excavation, the vertical stress increment concentrated at the pillars edges as shown in Fig. 5a. However, after longwall panels excavation, at the end of 1993 (the year of pillar burst) the vertical stress increment extended up to the pillars cores, especially in pillar RC2 as shown in Fig. 5b.

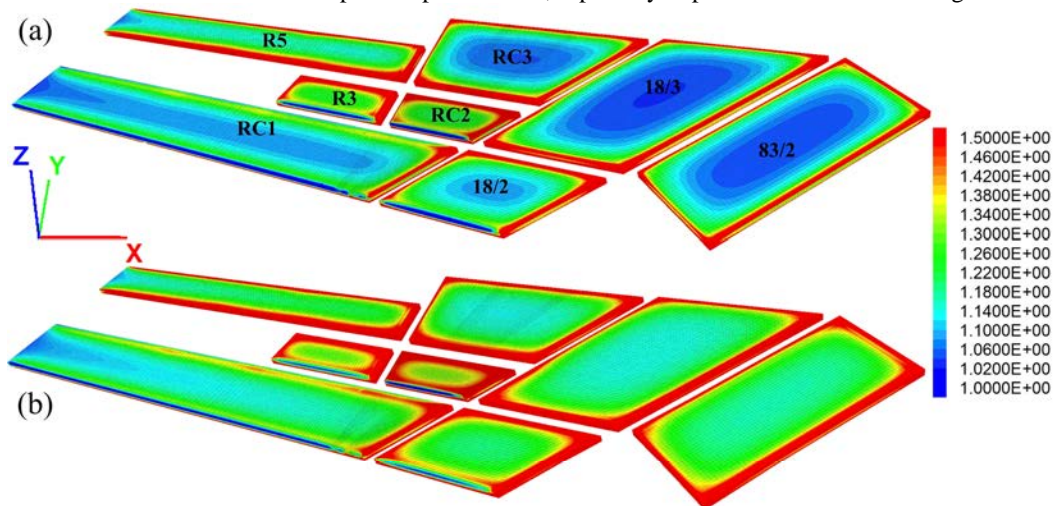


Fig.5. Normalized vertical stress distribution ( $\sigma_{zz}/\sigma_{zz(\text{ini})}$ ) (a) after excavation of shaft station galleries; (b) after panels excavation in 1993.

The main question is how these stress changes could lead to the failure of RC2 pillar? The elastic-perfect plastic mechanical behavior was applied to the coal pillars and strain-softening mechanical behavior was applied to the limestone seam at the middle of the coal pillars. The elasto-plastic calculation was performed to recognize the effect of longwall panels excavation in terms of plastic volume in the coal pillars. We noticed that the smallest pillar (RC2) gained the highest percentage of plastic zones at its edges due to excavations, where 30 % of the pillar imposed on plastic deformation. And, the largest pillar (RC1) gained the lowest percentage of plastic zones at its edge. Also, we found that the percentage of plastic zones did not increase due to longwall panels as shown in Fig. 6. The plasticized zones were kept almost constant after excavation of the shaft station galleries and the excavation of longwall panels (at the end of 1993). We also noticed that, the shear yield was the dominant and the tension failure appeared at the level of stiff limestone seam but it did not extend up to the pillar core as shown in Fig. 6.

As shown in Fig. 5, due to longwall panels exploitation, the stress increment reached up to the pillars cores, which could threaten their stability. The strength of RC2 pillar ( $\sigma_{ps} = 14$  MPa) could be estimated from Eq. (1) ( $w = 17.5$  m,  $h = 2.5$  m). The pillar strength is very low compared with its average stress (30 MPa). However, applying the elasto-plastic mechanical behavior on the shaft station area did not able to describe sufficiently this difference between the pillar average stress and the pillar strength in terms of plastic failure. For that, we used some rockburst criteria as a useful tool to explain the stress changes in terms of failure tendency.

By applying three different rockburst criteria, we found that the brittleness coefficient (B) criterion gave a constant value across all the shaft station pillars. The B value was found to be equal to 28 for the coal and 25 for the Limestone seam as shown in Table 1. These B values announce moderate rockburst tendency. But, this type of rockburst criterion that depend only on laboratory scale mechanical properties was found to be insufficient in case of large-scale excavations. Tao discriminant index ( $\alpha$ ) criterion produced a distribution similar to the maximum principal stress distribution. Tao index predicts a strong rockburst tendency ( $\alpha < 2.5$ ) for all shaft station pillars. On another hand, the Burst Potential Index (BPI) was able to distinguish between the pillars. The BPI varies from pillar to another as shown in Fig. 7. The BPI is almost 100% at the core of pillar RC2 (the smallest pillar) and 80 %



at the core of R3 pillar, while the other shaft station pillars have at maximum 50% BPI as shown in Fig. 7. The results obtained from the BPI distribution correspond the results obtained from applying the elasto-plastic behavior, where the pillars RC2 and R3 gained the highest percentage of plasticity at their edges. The Burst Potential Index (BPI) criterion was found to be a good tool to estimate the pillar burst tendency. But, the only disadvantage of this index (BPI) is that it depends on calculating the energy changes in one dimension only (the vertical direction). For that, further enhancement is required to adapt the BPI index in the 3D numerical calculations.

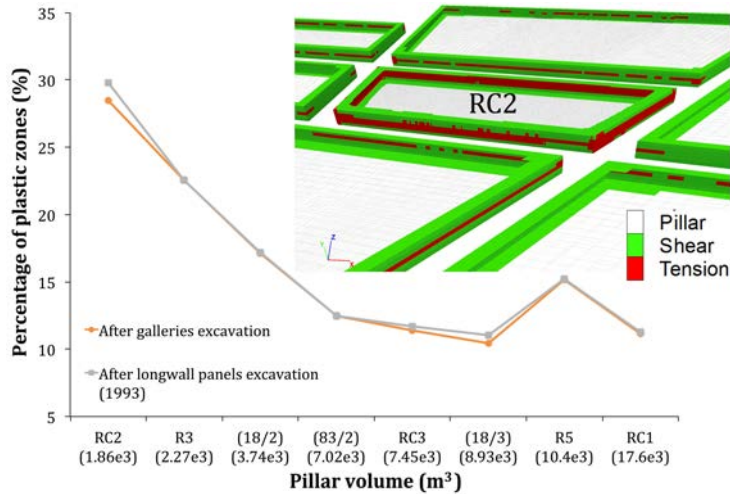


Fig. 6. Plasticity on shaft station pillars.



Fig. 7. Rockburst tendency at shaft station level (BPI criterion).

**5. Conclusion**

This paper presented a rockburst assessment based on large-scale numerical modeling. It examined the rockburst tendency at the shaft station of the Provence coal mine (France). The shaft station was excavated by using room-and-pillar mining method. This shaft station was surrounded by many panels excavated by longwall mining method. The longwall panels were excavated during 10 years between 1984 until 1994. A stiff limestone seam was recognized at the middle of coal pillars in the shaft station area. A pillar burst was recorded in the shaft station area in 1993. A 3D numerical model was constructed to simulate the longwall panels and the shaft station area to record the influence of large-scale excavations on pillars instability. Firstly, the shaft station galleries were excavated, then, the longwall panels were excavated.

We found that the vertical stress increased by 1.5 times its initial value. The vertical stress increment concentrated at the pillars edges after galleries excavations. But, this stress increment extended up to the core of the pillars after longwall panels excavations. Mohr-Coulomb mechanical model was performed to evaluate this stress increment in terms of plastic failure. We noticed that the smallest pillar gained the largest percentage of plasticity. The predominant yield type was the shear yield, and tension yield appeared at the level of the stiff limestone seam at the middle of coal pillars. However, the percentage of plastic zones did not increase due to longwall panels excavation. For that, we concluded that the perfect elasto-plastic mechanical model is not able alone to predict the rockburst or the pillars instability.

Three different rockburst criteria were implemented within the numerical model to test their ability to describe the failure tendency at the level of the shaft station area. These criteria were implemented in the numerical model of the Provence coal mine at the end of 1993 excavations. We found that, the criterion based on the laboratory values like the Brittleness coefficient ( $B$ ) gave constant rockburst tendency across all the shaft station pillars, which is not realistic and could not be applied on large-scale. Also, we found that the criteria that are based on stress changes like Tao discriminant index ( $\alpha$ ) criterion gave rockburst tendency distribution similar to that stress distribution. Finally, the criteria that are based on energy changes during excavations like the Burst Potential Index ( $BPI$ ) criterion gave a realistic burst tendency that corresponds to the stress and strain increment during excavations. The  $BPI$  was able to distinguish between the failed pillar and the other pillars. But, further enhancement is required to adapt the  $BPI$  index in the 3D.

More investigations are required in the numerical model of the Provence coal mine to observe the evolution of the stored train energy within the shaft station pillars during the longwall panels excavations. Also, other rockburst criteria could be implemented within the numerical model to observe their applicability in large-scale excavations.

## References

- [1] M.D.G Salamon, A.H Munro, A study of strength of coal pillars, J. Sth. Afr. Inst. Min. Metal. 68 (1967) 56–67.
- [2] C.S. Qiao, Z.Y. Tian, Study of the possibility of rockburst in Dong-gua-shan Copper Mine, Chinese J. Rock Mech. Eng. Žexp. 17 (1998) 917–921.
- [3] Z.H.U. Peng, Y. Wang, Griffith theory and the criteria of rock burs, Chinese J. Rock Mech. Eng. 17 (1996) 491–495.
- [4] C.A.I Meifeng, J. Wang, S. WANG, Analysis of energy distribution and prediction of rock burst during deep mining excavation in Linglong gold mine, Chinese J. Rock Mech. Eng. 20 (2001) 38–42.
- [5] N.R. Barton, R. Lien, J. Lunde, Engineering classification of rock masses for the design of tunnel support, Rock Mech. 6 (1974) 189–239.
- [6] Z.Y. Tao, Support design of tunnels subjected to rockbursting, in: Romana (Ed.), ISRM International Symposium, Rock Mechanics and Power Plants, 1988, pp. 407–411.
- [7] H.S. Mitri, B. Tang, R. Simon, FE modelling of mining-induced energy release and storage rates, J. Sth. Afr. Inst. Min. Metal. (1999) 103 - 110.
- [8] S. Ahmed, Numerical modeling of stress redistribution to assess pillar rockburst proneness around longwall panels: Case study of the Provence coal mine, France [Ph.D. thesis], Ecole des Mines de Nancy, France, 2016.
- [9] Z.T. Bieniawski, Strata control in mineral engineering, John Wiley&Sons, NewYork, Toronto, 1987, pp.135–146.
- [10] J.P. Tinucci, Analysis of pillar capacity in the vicinity of the Yvon Morandat shaft at U.E. Provence, Itasca consulting group report to unité d'exploitation Provence, December, 1993.
- [11] P. Gaviglio, P. Bigarre, H. Baroudi, J.P. Piguët, R. Monteau, Measurements of natural stresses in a Provence mine (Southern France), J. Eng. Geology. 44 (1996) 77–92.
- [12] S. Ahmed, Y. Gunzburger, V. Renaud, M. AlHeib, Initialization of highly heterogeneous virgin stress fields within the numerical modeling of large-scale mines, Int. J. Rock Mech Min. Sci. (2016).